Available online at www.sciencedirect.com
ScienceDirect
Tetrahedron
Tetrahedron 63 (2007) 1680–1688

New ICT probes: synthesis and photophysical studies of *N*-phenylaza-15-crown-5 aryl/heteroaryl oxadiazoles under acidic condition and in the presence of selected metal ions

Sabir H. Mashraqui,[a,*] Subramanian Sundaram[a] and A. C. Bhasikuttan[b]

[a]*Department of Chemistry, University of Mumbai, Vidyanagari, Santacruz-E, Mumbai 400098, India*
[b]*Radiation and Photochemistry Division, Bhabha Atomic Research Centre, Mumbai 400085, India*

Received 5 August 2006; revised 10 November 2006; accepted 30 November 2006
Available online 4 January 2007

Abstract—Molecular probes **6** and **7**, incorporating *N*-phenylaza-15-crown-5 and aryl/heteroaryl oxadiazole have been designed to function as the new intramolecular charge transfer (ICT) probes. Photophysical properties have been studied under acidic condition as well as in the presence of selected metal ions, Ca^{2+}, Ba^{2+}, Mg^{2+}, Na^{+}, K^{+}, and Li^{+}. The changes in the ICT character of the probes, following the addition of trifluoroacetic acid, were interpreted in terms of site and degree of protonations. Based on the cation affinity, the ICT bands in both UV–vis and emission spectra experienced varying degrees of blue shifts due to removal of the aza-crown ether nitrogen from conjugation. The cation-induced spectral shifts and the stability constants revealed binding strength in the order $Ca^{2+}>Ba^{2+}\gg Li^{+}>Na^{+}>K^{+}>Mg^{2+}$. Competitive experiments performed in a matrix of ions also indicated superior interaction of **6** and **7** with Ca^{2+}. The excited state decay profiles remained largely unperturbed in the presence of metal ions. The studied probes displayed positive solvatochromism and the Stokes shifts and excited state lifetimes increased with increasing solvent polarity. These findings can be rationalized by invoking highly polar nature of the emittive states. The chemoionophores **6** and **7** constitute potentially interesting Ca^{2+} sensitive probes due to their relatively high binding interaction for Ca^{2+} ($\log K_s$=3.55–3.10) vis-a-vis that of biologically interfering Mg^{2+} ($\log K_s$=1.67–1.30).

1. Introduction

There is a burgeoning interest in the design of molecular probes, which can selectively respond to traces of metal ions under various conditions.[1,2] Of the many techniques available for analyte detection, the cation-induced photophysical perturbations of chromo- and fluoroionophores constitute a very convenient and sensitive approach for the specific recognition of metal ions.[3] A variety of photophysical mechanisms, which govern the sensing phenomena include photo-induced electron transfer (PET), excimer/exciplex formation, photo-induced energy transfer, intramolecular charge transfer (ITC), and twisted intramolecular charge transfer (TICT). While PET and excimer/exciplex based systems generally produce signaling via fluorescence enhancement or quenching ('*on–off*' or '*off–on*' states), ICT probes could offer detection by modulation of both absorption and emission properties. Luminophores derived from naphthalene, anthracene, and pyrene principally operate as PET or excimer probes,[4] whereas chelating coumarins,[5] styryl dyes,[6] benzothiazole,[7] and 8-hydroxyquinoline[8] based chromophores have been employed in the majority of ICT systems. Notwithstanding the considerable progress reported in the area of optical molecular sensors, the quest for new molecular probes continues in order to improve both the selectivity and sensitivity of detection, particularly for common interfering analytes.

Photoemittive 2,5-diaryl-1,3,4-oxadiazoles find wide-spread applications as electronic and photonic materials,[9,10] however, applications as the signaling component in molecular sensory systems have only recently been described.[11] We were interested in targeting Ca^{2+} signaling because of its important role as an intracellular messenger in the regulation of cell functions.[12] In the context of our interest in metal ion sensors, we now describe the synthesis of two new chemoionophores **6** and **7**, and their photophysical behaviors under acidic conditions and in the presence of selected alkali (Li^{+}, Na^{+}, and K^{+}) and alkaline-earth cations (Ca^{2+}, Ba^{2+}, and Mg^{2+}). These cations, excluding barium, co-exist in the biological systems and are common interfering metal ions.[12]

Keywords: *N*-Phenylaza-15-crown-5 aryl/heteroaryl oxadiazole; Optical spectral studies; Alkali and alkaline-earth cations; Intramolecular charge transfer transition; Solvatochromism; Excited state lifetime.
* Corresponding author. Tel.: +91 22 26526091; fax: +91 22 26528547; e-mail: sh_mashraqui@yahoo.com

0040–4020/$ - see front matter © 2006 Published by Elsevier Ltd.
doi:10.1016/j.tet.2006.11.094

2. Results and discussion

2.1. Synthesis of 6 and 7 and the proposed binding mechanism

Aryl/heteroaryl 1,3,4-oxadiazoles were chosen as the photoemittive components and mono-aza-15-crown-5 as the cation receptor. The choice of mono-aza-15-crown-5 was dictated primarily by its known high affinity toward alkali and alkaline-earth metal ions, particularly calcium.[6a,13–16] The synthetic route implemented to access **6** and **7** is depicted in Scheme 1. Condensation of known *N*-phenylaza-15-crown-5 carboxaldehyde **1**[17] with the known 4-(*tert*-butylphenyl)hydrazide **2** or isoniazide **3** furnished the corresponding hydrazones **4** and **5**, respectively. Finally, oxidative cyclization using $KMnO_4$ in acetone[18] provided the target probes **6** and **7** in reasonable yields after SiO_2 column chromatographic purification. The structures are fully secured on the basis of elemental analysis and spectral data, which are summarized in Section 4.

In chromophores **6** and **7**, the receptor, *N*-phenylaza-crown and fluorophores, and aryl/pyridyl-oxadiazole components serve as an electron donor and electron acceptors, respectively. In analogy to known donor–acceptor chromophores, the ground and excited state properties of **6** and **7** are expected to be governed by an intramolecular charge transfer process.[3d,19] As illustrated in Scheme 2, cation coordination with the aza-crown domain of **6** or **7** would diminish the donor character of this ring, thereby curtailing the π-participation of the aza-crown nitrogen in conjugation.[3b,20] Consequently, the original CT character associated with **6** and **7** would be curtailed, a feature that should give rise to detectable changes in absorption and emission properties in the presence of interacting metal ions. Moreover, the presence of a π-deficient 4-pyridyl group in **7** should render the molecule a relatively stronger ICT system than **6** and hence the cation-induced photophysical perturbations for **7** are expected to be more pronounced than **6**.

2.2. Spectrophotometric investigation of 6 and 7 in the presence of trifluoroacetic acid

The absorption spectra of **6** and **7** measured in acetonitrile are shown in Figures 1 and 2, respectively. The spectra displayed a weak, higher energy band in the range of 255–278 nm and a relative strong absorption in the range of 338–351 nm. The former band is attributable to a locally excited transition (LE), while the lower energy absorption can be assigned to an intramolecular charge transfer transition. In agreement with our proposition, a higher degree of ICT character in **7** compared to that of **6** is clearly evident from a relatively lower energy of the ICT band associated with **7** (λ_{ICT} 351 vs 338 nm for **6**).

The spectrophotometric properties of **6** and **7**, carrying basic site(s) are expected to be sensitive to acid. Accordingly, to see the effect of acid, the absorption spectra of **6** or **7** were

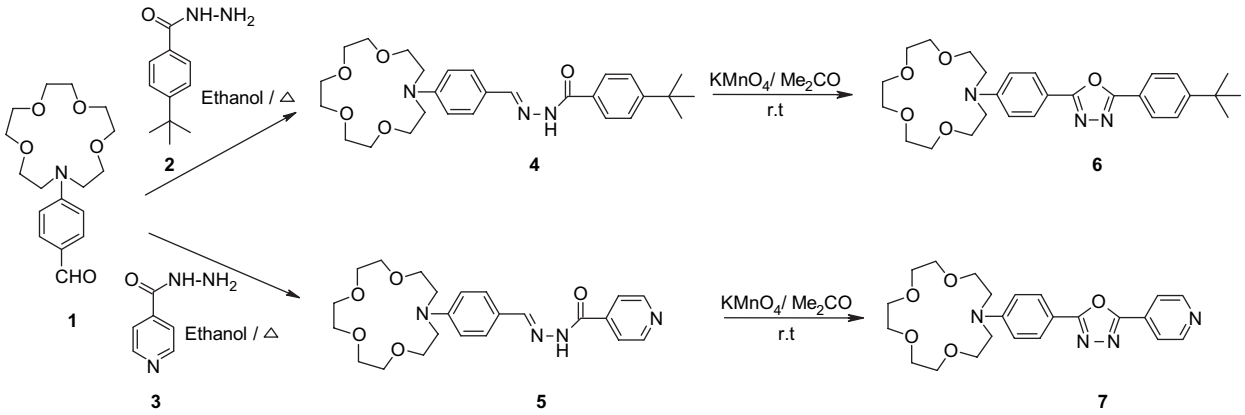

Scheme 1. Synthetic routes for chemoionophores **6** and **7**.

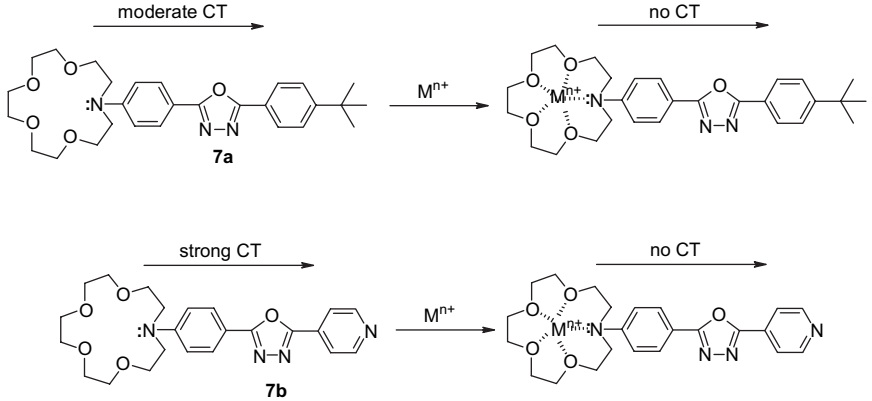

Scheme 2. Proposed charge transfer (CT) interaction of **6** and **7** with metal ion (M^{n+}).

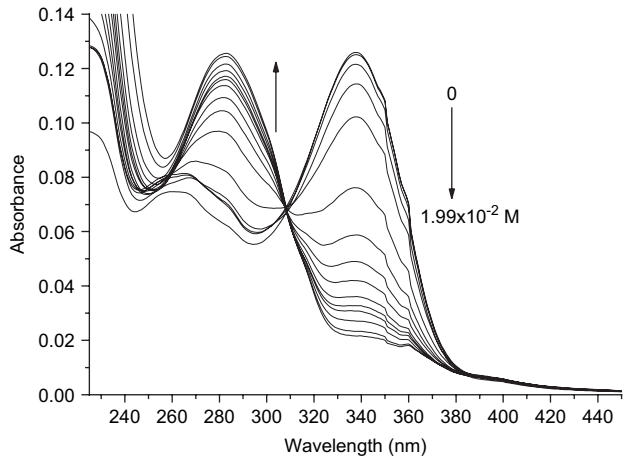

Figure 1. Absorption spectra of **6** (3.29×10^{-6} M) on titration with TFA (0–1.99×10^{-2} M in CH_3CN).

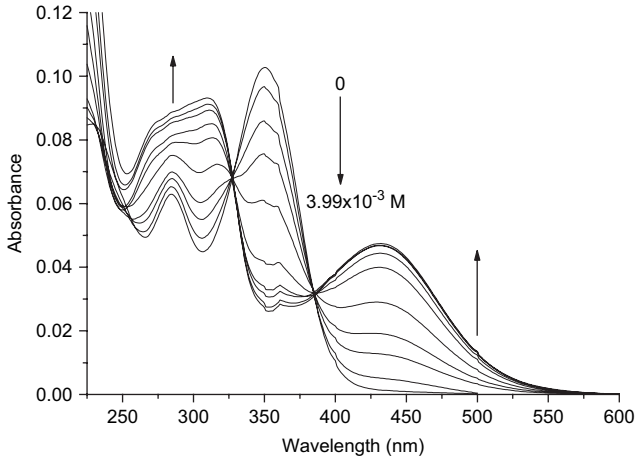

Figure 2. Absorption spectra of **7** (3.28×10^{-6} M) on titration with TFA (0–3.99×10^{-3} M in CH_3CN).

recorded by titrating their fixed concentration with incremental additions of trifluoroacetic acid (TFA) (0–1.99×10^{-2} M in acetonitrile). For **6**, addition of TFA resulted in the complete disappearance of the original ICT band, while a new hypsochromically shifted band emerged at 285 nm with a clear isosbestic point at 308 nm (Fig. 1). The disappearance of the ICT band is readily ascribed to the formation of **6**+H^+ in which the aza-crown nitrogen lone pair is no longer available for the electronic delocalization.[7d,21] The pK_a of **6** determined in 1:1 methanol–water by plotting absorbance versus pH was found to be ca. 3.2 (±0.1) and for the parent *N*-phenylaza-15-crown-5 it was found to be ca. 4.9 (±0.1). The reduced basicity of the aza-crown nitrogen in **6** compared to the reference, *N*-phenylaza-15-crown-5 is understandable in view of electron withdrawing character of the conjugated oxadiazole chromophore.[22,23]

In contrast to **6**, for the case of **7**, protonation in principle, can occur not only at the aza-crown nitrogen but also at the pyridyl nitrogen or at both of these positions. However, it should be possible to ascertain the site of protonation(s) on the basis of the resultant spectral changes of **7** in the presence of added acid. In the event, addition of TFA (0–3.99×10^{-3} M) to a CH_3CN solution of **7** resulted in a progressive decrease in the intensity of the original ICT band at 351 nm, with concomitant emergence of one bathochromically (λ_{max} 432 nm) and another hypsochromically (λ_{max} 311 nm) shifted bands. Formation of two new absorption maxima implies that more than one protonated derivative of **7** is involved. As illustrated in Scheme 3, the red shifted absorption is clearly a consequence of the protonation of the pyridyl nitrogen to form **7**-py-H^+ in which increased electronic delocalization from the aza-crown nitrogen leads to enhanced ICT interaction relative to neutral **7**. On the other hand, the blue shifted absorption could arise from the competitive protonation of aza-crown nitrogen to form **7**-aza-H^+. The basicities of *N*-phenylaza-15-crown-5 and that reported for pyridine are quite similar (pK_a 4.9 vs 5.23).[24] Assuming that the ground state pK_a of the basic

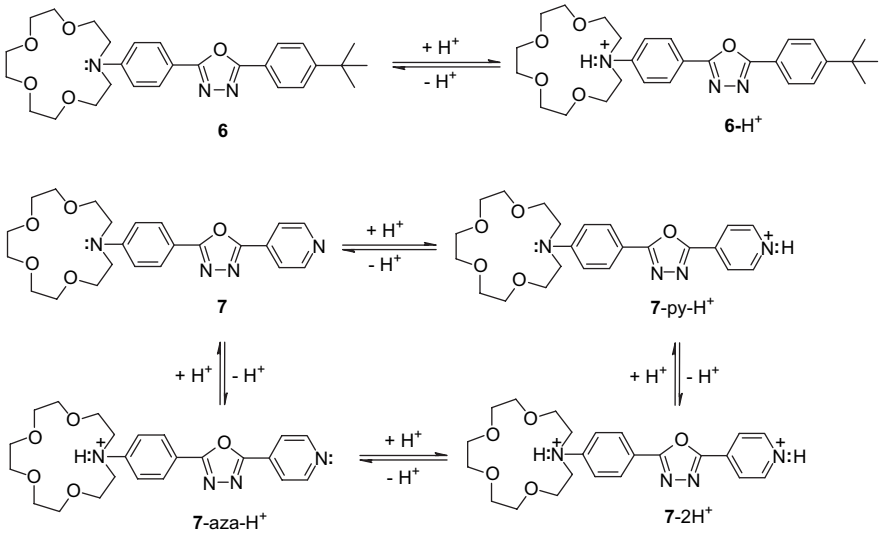

Scheme 3. Proposed protonation equilibria involving **6** and **7**.

centers is not appreciably altered due to π-conjugation, then there may not be much to choose between for protonation of the aza-crown nitrogen and the pyridyl nitrogen. Under such circumstance, dual protonation generating both **7**-py-H^+ and **7**-aza-H^+ species may not be entirely unexpected. Similar spectral behavior has also been reported by Mitewa et al. in aza-15-crown-5-styryl benzothiazole under acidic condition, which also exhibited simultaneous protonation on the aza-crown and benzothiazole nitrogens.[25] At high TFA concentration (9.99×10^{-2} M) the red shifted band is completely replaced by the blue shifted band, signaling the formation of only bis-protonated species, **7**+$2H^+$. Unfortunately, due to complicated equilibria involved in the protonation(s) of **7**, we were unable to accurately determine its pK_a values.

Excitation of **6** and **7** in acetonitrile at their λ_{max} produced emissions at 438 and 550 nm, respectively. The quantum yields (Φ_f) of **6** and **7** were calculated to be 0.528 and 0.288, respectively, based on comparison with the integrated fluorescence spectra of the reference standard, coumarin 153 in cyclohexane (Φ_f=0.90).[26] Relatively lower Φ_f and higher Stokes shifts for **7** (199 vs 100 nm for **6**) are consistent with its relatively higher ICT character, which turns the molecule largely non-radiative in nature.[27,28]

As expected, the fluorescent emissions were also modified in the presence of TFA. Upon titration of **6** with TFA, a new, more intense blue shifted emission band appeared at 363 nm (blue shift of ca. 75 nm) at the expense of original ICT emission centered at 438 nm (Fig. 3). The blue shift in the emission is consistent with the absorption spectra, which are also similarly affected by protonation on the aza-crown nitrogen. In the case of **7**, the fluorescence spectra were dependent upon the chosen excitation wavelength in the presence of TFA. Excitation at 325 nm (isosbestic point closer to the LE state, Fig. 4) produced a blue shifted emission at 410 nm, down from 550 nm observed for neutral **7**. The blue shifted emission, which increased in intensity with increasing acid concentration can be assigned to the local emission stemming from either the mono-protonated form in which only the aza-crown nitrogen is protonated (**7**-aza-H^+) and/or the bis-protonated species (**7**-$2H^+$).

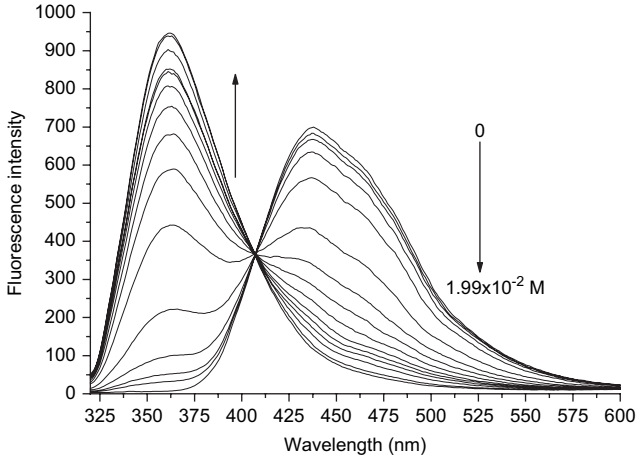

Figure 3. Fluorescence spectra of **6** (3.29×10^{-6} M, λ_{ex}=308 nm) on titration with TFA (0–1.99×10^{-2} M in CH_3CN).

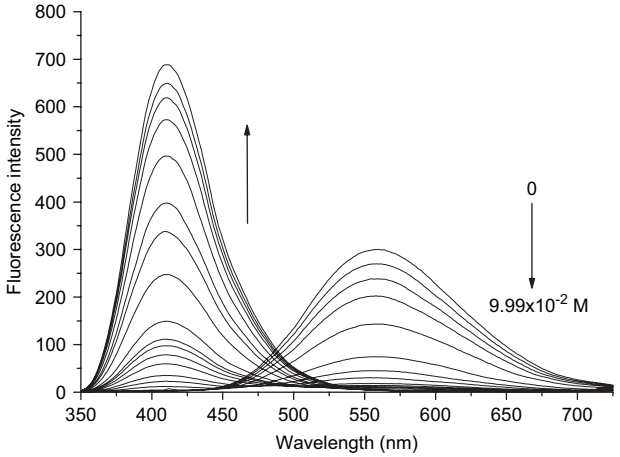

Figure 4. Fluorescence spectra of **7** (3.28×10^{-6} M; λ_{ex}=325 nm) on titration with TFA (0–9.99×10^{-2} M in CH_3CN).

On the other hand, the excitation of **7** at 386 nm (isosbestic point closer to the CT state) led to the development of a slightly red shifted emission at 556 nm (for neutral **7**, the λ_{em} is centered at 550 nm) due to the formation of the **7**-py-H^+ form (Scheme 3). This emission showed progressive decline in intensity with increasing TFA concentration (Fig. 5). The non-emissive nature of this species is in accord with several known anilino donor–acceptor systems, viz. dialkylaminopyridine, 2-(4-dialkylanilino)benzothiazole and *N*-phenylaza-crown styryl-benzothiazole, which also form non-emissive ICT species on protonation.[29]

2.3. Spectrophotometric investigation of 6 and 7 in the presence of metal ion perchlorates

The effects of the addition of various metal perchlorates on the UV–vis profiles of **6** and **7** are depicted in Figures 6 and 7, respectively, and the spectrophotometric data in the absence and presence of metal ions are summarized in Table 1. Metal ion concentrations required to achieve complete complexation are also indicated in Figures 6 and 7. Addition of Li^+, Na^+, and K^+ perchlorates resulted in small (3–9 nm) hypsochromic shifts of the ICT band of **6**, whereas Mg^{2+} produced no change in the energy of the ICT band, but

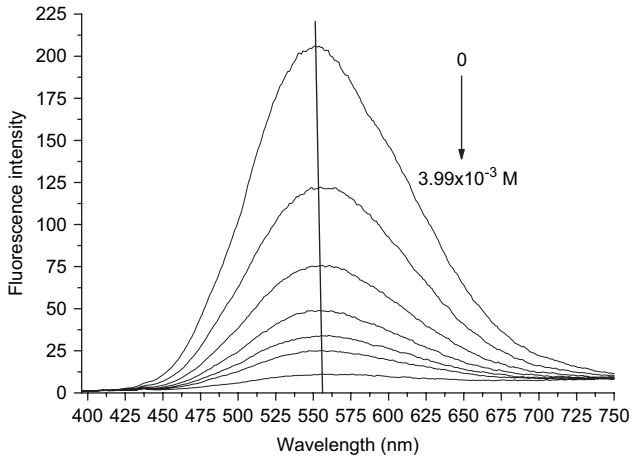

Figure 5. Fluorescence spectra of **7** (3.28×10^{-6} M; λ_{ex}=386 nm) on titration with TFA (0–3.99×10^{-3} M in CH_3CN).

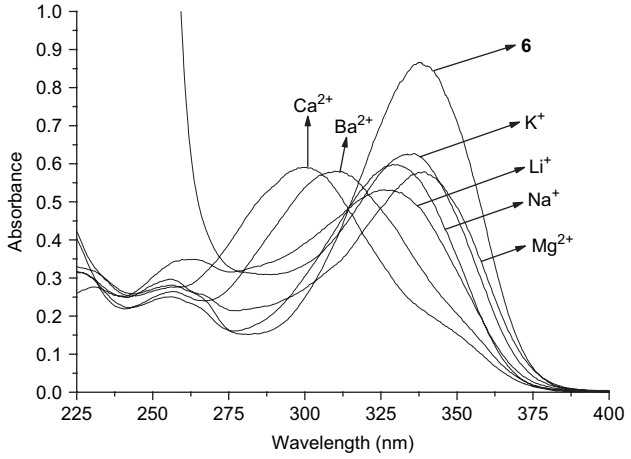

Figure 6. Absorption spectra of **6** (2.27×10^{-5} M) in CH_3CN and **6** containing Ca^{2+} (4.54×10^{-3} M), Ba^{2+} (1.02×10^{-2} M), Mg^{2+} (3.40×10^{-2} M), Li^+ (2.30×10^{-2} M), Na^+ (2.91×10^{-2} M), and K^+ (4.10×10^{-2} M).

only a slight decrease in the band intensity. These results suggest insignificant interaction of Li^+, Na^+, K^+, and Mg^{2+} ions with **6**. On the other hand, UV–vis spectra of **6** were more significantly perturbed in the presence of Ca^{2+} and Ba^{2+} perchlorates, as evidenced by the relatively larger blue shifts of 38 and 28 nm, respectively, in the original ICT band. For the case of **7** also Li^+, Na^+, K^+, and Mg^{2+} led to smaller blue shifts (1–11 nm), while Ca^{2+} and Ba^{2+} produced more pronounced blue shifts of 59 and 40 nm, respectively. With all the metal ions examined, the blue shifts in ICT bands were accompanied by decreases in the intensity of this transition. Such anti-auxochromic effects are well documented in aza-crown chromophores wherein the cations bind at the donor site.[17,30,31]

The superior interaction of Ca^{2+} (and to a lesser extent with Ba^{2+}) results in the strong decoupling of aza-crown nitrogen lone pair from conjugation, causing a much larger decrease in the ICT character and hence a strong blue shift in the absorption maxima. The stability constant, log K_s, was determined from spectrophotometric titration carried out by

Table 1. UV–vis data of free and complexed ligands **6** and **7**

Complex	**6**			**7**		
	λ_{ICT}^{max} (nm)	$\Delta\lambda_{ICT}$ (nm)	ϵ_M (L mol^{-1} cm^{-1})	λ_{ICT}^{max} (nm)	$\Delta\lambda_{ICT}$ (nm)	ϵ_M (L mol^{-1} cm^{-1})
Neat	338	—	38,283	351	—	31,008
Ca^{2+}	300	38	26,127	292	59	23,397
Ba^{2+}	310	28	25,696	311	40	20,176
Mg^{2+}	337	1	25,386	350	1	19,911
Li^+	329	9	23,493	342	9	19,792
Na^+	330	8	26,454	340	11	19,972
K^+	335	3	27,749	347	4	25,388

incremental addition of metal salts dissolved in acetonitrile (up to maximum complexation) into a fixed concentration of chromophores **6** and **7**. As shown for the binding of Ca^{2+} ions with **6** (Fig. 8), a well-defined isosbestic point is observed. By applying the Job's plot,[32] 1:1 binding stoichiometry of complexation was confirmed (Fig. 9). The log K_s calculated by non-linear curve fitting method[32] is listed in Table 2. The log K_s is in conformity with the magnitude of the observed hypsochromic shifts and the binding interaction follows the order $Ca^{2+}>Ba^{2+}\gg Li^+>Na^+>K^+>Mg^{2+}$. Although, the hypsochromic shifts with metal salts are higher for **7** than **6**, however, the stability constants for **7** are comparatively lower than **6**. This is understandable in view of the presence of an electron withdrawing pyridyl group, which serves to reduce the binding ability of **7**. Available comparisons indicate that log K_s derived from our systems is comparable with the binding constants reported for some known *N*-phenylaza-15-crown-5 dyes[13] (Table 2).

In order to evaluate the selective binding of Ca^{2+}, we performed a competitive spectral analysis in the presence of a matrix of ions (Fig. 10). Initially, a UV–vis spectrum of **6** (2.27×10^{-5} M) in the presence of a mixture of Ba^{2+} (1.02×10^{-2} M), Li^+, Na^+, K^+, and Mg^{2+} ions (each 4×10^{-2} M) was recorded. The resultant spectrum showed an absorption band at 310 nm, which matches with the spectrum obtained in the presence of Ba^{2+} alone (cf. Fig. 6). This result shows that Ba^{2+} interacts more strongly than Li^+, Na^+, K^+, and Mg^{2+} ions. Upon titrating the above solution against the incremental addition of calcium

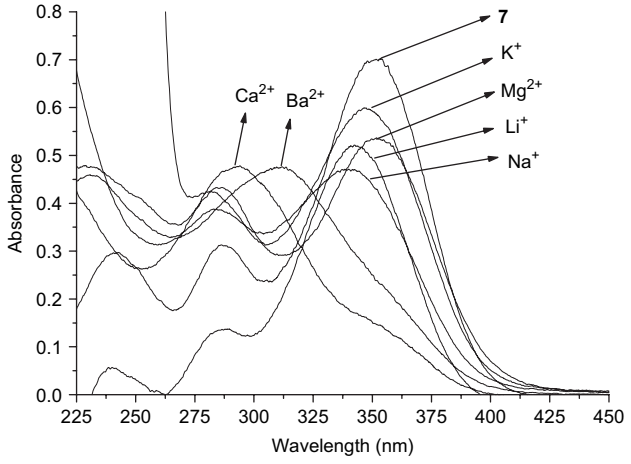

Figure 7. Absorption spectra of **7** (2.27×10^{-5} M) in CH_3CN and **7** containing Ca^{2+} (9.1×10^{-3} M), Ba^{2+} (1.36×10^{-2} M), Mg^{2+} (3.63×10^{-2} M), Li^+ (2.61×10^{-2} M), Na^+ (2.90×10^{-2} M), and K^+ (4.2×10^{-2} M).

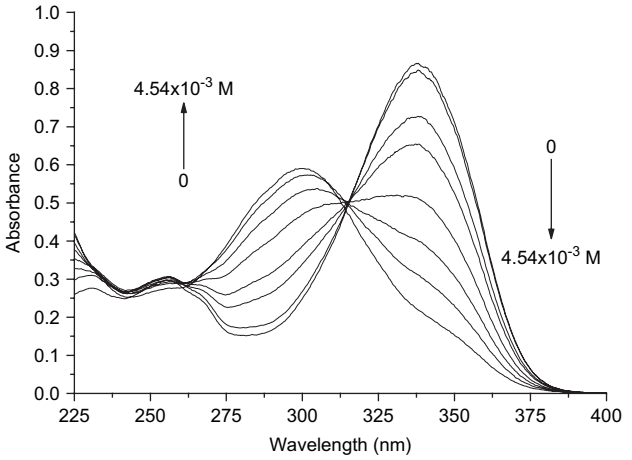

Figure 8. Absorption spectra of **6** (2.27×10^{-5} M) in CH_3CN in the presence of increasing amount of $Ca(ClO_4)_2$ up to 4.54×10^{-3} M (saturation point).

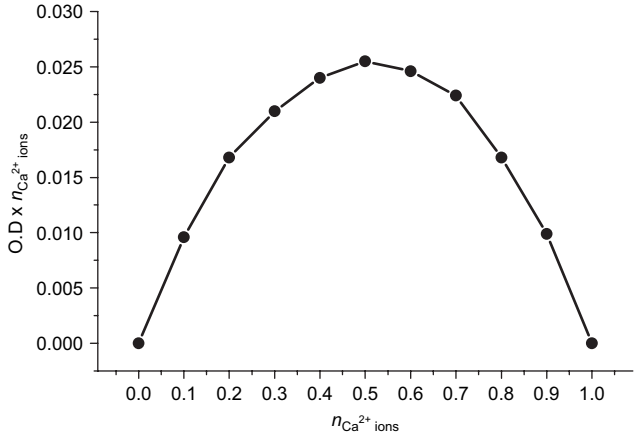

Figure 9. Job's plot for the **6**+Ca^{2+} complex.

perchlorate (0–5×10^{-3} M), the 310 nm band is gradually blue shifted to form an entirely new band at 300 nm. The latter band is clearly due to the exclusive formation of **6**+Ca^{2+} complex (cf. Fig. 6). This competitive experiment serves to demonstrate the superior binding affinity of **6** with Ca^{2+} ions relative to alkali and other alkaline-earth metal ions examined. Similar behavior was also noticed for **7**, which showed that in the matrix of ions, Ca^{2+} is more selectively complexed. It is noteworthy that chromoionophores **6** and **7** exhibit relatively stronger association with Ca^{2+} (log K_s= 3.55–3.10) over that of a common, interfering Mg^{2+} ion (log K_s=1.67–1.30).

The stronger binding of Ca^{2+} ion is in accord with its ionic diameter of 1.98 Å, which is complimentary to the cavity size of the aza-crown ether (1.7–2.2 Å).[33] However, Na^+ despite its ionic radii (1.94 Å) being comparable to that of Ca^{2+} ion displayed much poor affinity than Ca^{2+}. Similar behavior was also observed by Moore and Lewis[13] and Valeur et al.[31] with some aza-crown chromophores and is ascribed to higher charge density and larger gain in entropy associated with desolvation of Ca^{2+} over that of Na^+. Optimal size-fit concept alone does not account for the superior binding of the much smaller lithium ion (ionic radii 1.52 Å) than Na^+. Rurack et al. have also encountered similar results in the binding studies of some aza-crown chalcones and proposed that extensive solvation of the smaller Li^+ (Na^+ as well as K^+ ions) could lead to solvated lithium ions, which could thus exhibit a better fit in the larger aza-crown cavity.[7a,34]

2.4. Fluorescence spectral studies of 6 and 7 before and after metal ion additions

On the addition of alkali and alkaline-earth metal ions, the fluorescence intensity of **6** remained practically unchanged.

Table 2. Stability constants (log K_s) of metal complexes of **6** and **7**

M^{n+}	Ionic diameter (Å)	log K_s (**6**+M^{n+})	log K_s (**7**+M^{n+})	Ranges of log K_s for known (*N*-15-C-5 dyes)[13]
Li^+	1.36	2.14	1.90	1.7–2.8
Na^+	1.94	1.94	1.77	1.4–2.2
K^+	2.66	1.07	0.54	1.3–2.2
Mg^{2+}	1.32	1.67	1.30	1.6–2.98
Ca^{2+}	1.98	3.55	3.10	1.7–4.2
Ba^{2+}	2.68	3.03	2.89	1.9–3.6

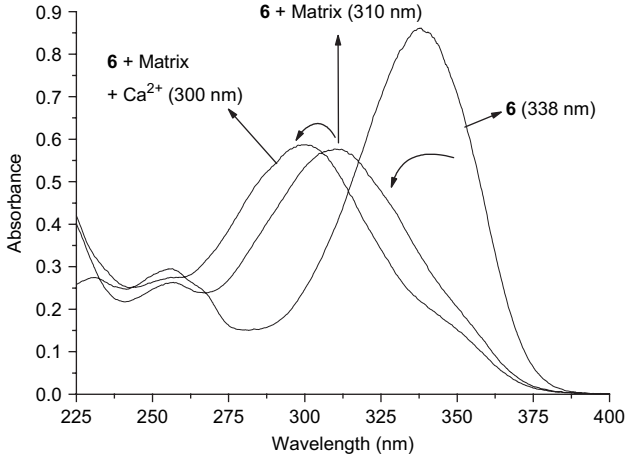

Figure 10. Absorption spectra of **6** (2.27×10^{-5} M), **6**+matrix [Ba^{2+} (1.02×10^{-2} M), Mg^{2+}, Li^+, Na^+, and K^+ (4×10^{-2} M), each], and **6**+matrix+Ca^{2+} (5×10^{-3} M) in CH_3CN.

However, the λ_{em} suffered marginal blue shifts on addition of perchlorates of Ca^{2+} ($\Delta\lambda$ 10 nm), Ba^{2+} ($\Delta\lambda$ 8 nm), and Li^+ ($\Delta\lambda$ 6 nm). In the presence of weaker complexing K^+, Na^+, and Mg^{2+} ions, no perceptible changes were detected in the λ_{em} (Fig. 11). Thus, in accord with the results obtained earlier from the absorption spectra, the emission spectral changes also indicated the binding interaction to follow the order: Ca^{2+}>Ba^{2+}≫Li^+>Na^+>K^+>Mg^{2+}. Similar spectral behavior was exhibited by **7**, but the magnitude of cation-induced blue shifts were comparatively higher (Ca^{2+}, 19 nm; Ba^{2+}, 14 nm; Li^+, 10 nm; Na^+, 3 nm; K^+, 1 nm; Mg^{2+}, 4 nm). The fluorescence spectral changes for **6** and **7** are shown in Figures 11 and 12, respectively, and the photophysical data are summarized in Table 3.

It is noteworthy that the blue shifts in the λ_{ICT} of **6** and **7** in the presence of metal ions are substantially larger than that of the corresponding shifts observed in their fluorescence emission spectra. The much reduced levels of blue shifts in the emission spectra imply relatively weaker cation–aza crown interaction in the excited states compared to the

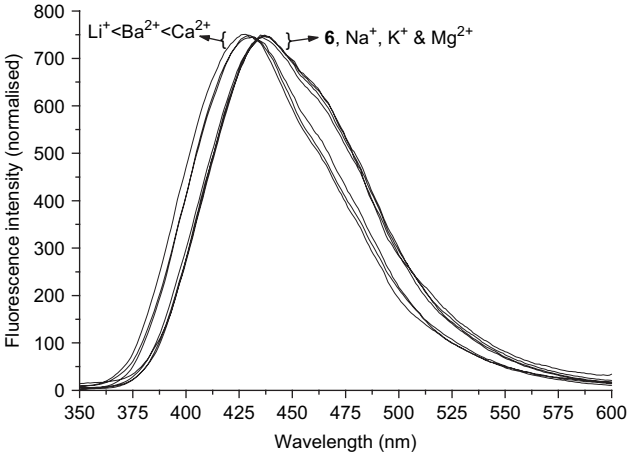

Figure 11. Fluorescence spectra (corrected) of **6** (3.29×10^{-6} M) in CH_3CN and **6** containing Ca^{2+} (6.58×10^{-4} M), Ba^{2+} (1.48×10^{-3} M), Mg^{2+} (4.93×10^{-3} M), Li^+ (3.29×10^{-3} M), Na^+ (4.27×10^{-3} M), and K^+ (5.92×10^{-3} M).

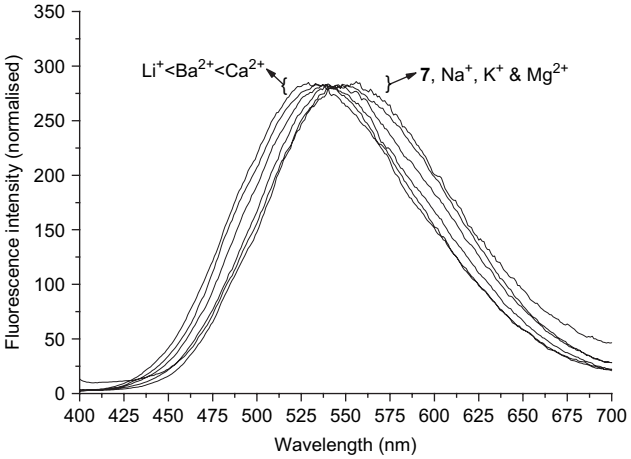

Figure 12. Fluorescence spectra (corrected) of **7** (3.28×10^{-6} M) in CH_3CN and **7** containing Ca^{2+} (1.31×10^{-3} M), Ba^{2+} (1.97×10^{-3} M), Mg^{2+} (5.25×10^{-3} M), Li^{+} (3.77×10^{-3} M), Na^{+} (4.26×10^{-3} M), and K^{+} (6.07×10^{-3} M).

ground states. Reduced complexation in the excited states is also indicated by the fluorescence lifetime profiles of **6** and **7** in the presence of metal ions. As shown in Table 3, no significant changes were observed in the lifetimes of **6** and **7** in the presence of various metal ions, thereby implying that emissions occur largely from the de-complexed molecules. Precedence for such metal–ligand decomplexations in the excited states has been earlier documented in aza-crown donor–acceptor and related systems.[2,35,36]

2.5. Solvatochromic and excited state lifetime profiles

In analogy to typical donor–acceptor chromophoric systems, the ground and excited state properties of chemoionophores **6** and **7** were found to be markedly influenced by the polarity of solvents.[37] The absorption and emission data measured in different solvents together with excited state lifetimes are summarized in Table 4.

Both **6** and **7** were found to exhibit positive solvatochromism. As can be seen from Table 4, the effects of solvent polarity on the absorption maxima corresponding to the ICT transition are less marked with a red shift in λ_{ICT} amounting to only 6–7 nm in going from apolar hexane to the more polar methanol. In contrast, emission energies were significantly modified for both **6** and **7** with increasing solvent polarity. Thus, when excited at their respective absorption maxima, structureless ICT emissions showing increasing red shifts in more polar solvents were observed.[7a,28,38] For

Table 3. Fluorescence data and excited state lifetime (τ_F) of free and complexed ligands **6** and **7**

Complex	**6**			**7**		
	λ_{em} (nm)	$\Delta\lambda_{em}$ (nm)	τ_F (ns)	λ_{em} (nm)	$\Delta\lambda_{em}$ (nm)	τ_F (ns)
Neat	438	—	2.28	550	—	3.75
Ca^{2+}	428	10	2.20	531	19	3.29
Ba^{2+}	430	8	2.05	536	14	3.70
Mg^{2+}	436	2	2.35	546	4	3.05
Li^{+}	432	6	2.23	540	10	3.49
Na^{+}	436	2	2.28	547	3	3.39
K^{+}	437	1	2.28	549	1	3.34

Table 4. Solvatochromic and τ_F of **6** and **7** in various solvents

Solvent	**6**			**7**		
	λ_{abs} (nm)	λ_{em} (nm)	τ (ns)	λ_{abs} (nm)	λ_{em} (nm)	τ_F (ns)
Hexane	334	382	1.14	350	402	1.39
Diethyl ether	336	398	1.39	350	439	2.98
Chloroform	340	405	1.19	356	477	3.90
Ethyl acetate	337	411	1.63	351	490	3.92
Acetonitrile	338	440	2.28	351	551	4.31
Methanol	341	442	2.94	356	578	[a]

[a] Fluorescence lifetime could not be determined due to fluorescence quenching.

the case of **6**, the emission band was red shifted from 382 nm in hexane to 442 nm in methanol, while for **7**, the emission band was red shifted from 402 nm in hexane to 578 nm in methanol. These finding are characteristic of the polar nature of the emissive excited states for both **6** and **7**, which get significantly stabilized compared to their ground states. The emission then occurs from highly relaxed Frank–Condon states so as to produce red shifted emissions in more polar solvents. As expected on the ground state of the higher ICT character, the polarity-induced Stokes shifts for **7** are relatively more pronounced (maximum $\Delta\lambda_{em}$ 176 nm) than that observed for **6** (maximum $\Delta\lambda_{em}$ 60 nm).[39,40] Such pronounced solvent-induced Stokes shifts observed with the ICT probe **7** might be of potential interest to study the medium effects in chemical and biological systems.[2]

The lifetime decay profile predominantly followed a single exponential decay function (consisting of a single species, up to 97% photoemittive state) and the lifetime of ICT emittive state displayed increasingly longer lifetimes in solvents of higher polarity. This result reflects a greater stabilization of the ICT emittive state in going from less polar hexane to more polar methanol. Alternatively, the highly polar nature of fluorescence can also be reconciled by invoking twisted intramolecular charge transfer (TICT) states.[28] Whether the excited state photophysical properties are due to the ICT or TICT states must await a critical analysis of the solvatochromic data, including solvent dependent quantum yields. Work along this line is underway in our laboratory.

3. Conclusions

Photophysical properties of newly synthesized ICT probes **6** and **7** are mediated by ICT mechanisms under different conditions. The absorption and emission spectral shifts experienced by **6** and **7** in the presence of TFA arise due to a decrease or increase in the ICT character depending upon the site and degree of protonation(s). The magnitude of the absorption and emission blue shifts and stability constants revealed the binding strength to follow the order $Ca^{2+}>Ba^{2+}\gg Li^{+}>Na^{+}>K^{+}>Mg^{2+}$. Titration experiments in a matrix of ions also indicated superior binding of Ca^{2+}. Available evidence suggests that metal ion binding in the excited states is weaker than that in the ground state. The chromophores displayed positive solvatochromism and their excited state lifetimes increased with increasing solvent polarity. These findings can be attributed to the highly polar nature of the emittive states. Significantly high solvent-induced Stokes shifts for the ICT probe **7** might be exploited

to study medium effects in biological and other systems. Relatively high spectral shifts and binding constants demonstrated by the ICT probes with Ca^{2+} (log K_s=3.55–3.10), compared to the biologically interfering Mg^{2+} (log K_s= 1.67–1.30) and alkali metal ions (log K_s=0.54–2.14) are of potential interest from the chemosensors' perspective.

4. Experimental

4.1. General

The chemicals and spectral grade solvents were purchased from S.D. fine Chemicals (India) and used as received. IR spectra were recorded on a Shimadzu FTIR-420 spectrophotometer. ^{1}H NMR spectra were recorded in $CDCl_3$ solution on a Bruker 300 MHz spectrometer with TMS as an internal standard. Coupling constants *J* are given in hertz. ^{13}C NMR spectra (75.5 MHz) were recorded on a Bruker AC 300 instrument. Mass spectra were obtained using LC–MS in ESI mode. Elemental analyses were done on Carlo Erba instrument EA-1108 Elemental analyzer. UV–vis spectra were recorded on Jasco V-530 UV–vis spectrophotometer, fluorescence spectra were recorded on Hitachi F-4500 Fluorescence spectrophotometer, and fluorescence lifetime measurements were recorded on E1-199 Fluorescence spectrometer.

4.1.1. Preparation of hydrazone 4. The known *N*-phenylaza-15-crown-5 carboxaldehyde **1** (1.29 g, 4 mmol)[17] and 4-*tert*-butylbenzoic hydrazide **2** (0.768 g, 4 mmol)[41] were dissolved in absolute ethanol (20 mL) and refluxed on a water-bath for about 3 h. The reaction mixture was then cooled to room temperature and the precipitated solid filtered, washed with cold ethanol, and air dried to obtain the product **4** as a pale yellow solid in 80% yield (1.59 g), mp 160–162 °C. IR (KBr, ν, cm^{-1}): 3192, 3011, 2953, 2867, 1640, 1609, 1593, 1521, 1355, 1304, 1183, 1117, 1060, 814, 731. ^{1}H NMR (300 MHz, $CDCl_3$): δ 9.90 (s, 1H), 8.22 (s, 1H), 7.83 (d, *J*=6.5 Hz, 2H), 7.57 (d, *J*=7 Hz, 2H), 7.41 (d, *J*=6.5 Hz, 2H), 6.62 (d, *J*=7 Hz, 2H), 3.74 (t, 4H), 3.64–3.61 (m, 16H), 1.29 (s, 9H). ^{13}C NMR ($CDCl_3$): δ 164.04, 155.25, 149.377, 149.09, 130.53, 129.59, 127.24, 125.57, 121.53, 111.67, 71.16, 70.21, 70.01, 68.25, 52.84, 34.96, 31.16. *m/z*: 497 (M^+), 464, 439, 408, 364, 350, 346, 319, 304, 291, 276, 190, 174, 165, 138, 132, 118, 90, 77, 57. Anal. Calcd for $C_{28}H_{39}N_3O_5$: C, 67.60; H, 7.80; N, 8.45. Found: C, 67.80; H, 8.10; N, 8.70%.

4.1.2. Synthesis of 2-(4-*N*-phenylaza-15-crown-5)-5-(4-*tert*-butylphenyl)-1,3,4-oxadiazole (6). To a stirred solution of Schiff base **4** (0.994 g, 2 mmol) in dry acetone (50 mL) was added $KMnO_4$ (0.994 g) portionwise during 1 h and the reaction continued to be stirred at room temperature for another 4 h whereby the pink reaction mixture changed to dark brown color. The reaction mixture was then filtered and the filtrate concentrated to get a crude solid. The crude product was purified by SiO_2 column chromatography (eluant: 1% CH_3OH in $CHCl_3$) to obtain the desired product **6** as a white solid in 65% yield (0.643 g), mp 94–96 °C. IR (KBr, ν, cm^{-1}): 2869, 1611, 1502, 1354, 1193, 1125, 957, 842, 752, 665. ^{1}H NMR (300 MHz, $CDCl_3$): δ 8.03 (d, *J*=9 Hz, 2H), 7.94 (d, *J*=9 Hz, 2H), 7.52 (d, *J*=9 Hz, 2H), 7.75 (d, *J*=9 Hz, 2H), 3.80 (t, 4H), 3.69–3.64 (m, 16H), 1.37 (s, 9H). ^{13}C NMR ($CDCl_3$): δ 164.98, 163.60, 154.73, 150.04, 128.47, 126.53, 125.93, 121.61, 111.41, 111.03, 71.33, 70.30, 70.09, 68.29, 52.72, 35.04, 31.16. *m/z*: 495 (M^+), 350, 320, 306, 291, 174, 160, 138, 131, 118, 91, 77, 57. Anal. Calcd for $C_{28}H_{37}N_3O_5$: C, 67.88; H, 7.47; N, 8.48. Found: C, 68.03; H, 7.67; N, 8.78%.

4.1.3. Preparation of hydrazone 5. Following the procedure described for **4**, the condensation of **1** (1.292 g, 4 mmol) with isoniazide **3** (0.548 g, 4 mmol) gave the hydrazone **5** as a pale yellow solid in 85% yield (1.503 g), mp 205–207 °C. IR (KBr, ν, cm^{-1}): 3191, 3037, 2860, 1646, 1594, 1519, 1392, 1357, 1299, 1183, 1115, 1067, 991, 921, 813, 682. ^{1}H NMR (300 MHz, $CDCl_3$): δ 10.99 (s, 1H), 8.63 (d, *J*=7.5 Hz, 2H), 8.36 (s, 1H), 7.84 (d, *J*=7.5 Hz, 2H), 7.46 (d, *J*=9 Hz, 2H), 6.53 (d, *J*=9 Hz, 2H), 3.69 (t, 4H), 3.62–3.56 (m, 16H). ^{13}C NMR ($CDCl_3$): δ 162.03, 151.51, 149.67, 141.36, 129.67, 123.93, 121.81, 120.65, 111.31, 71.16, 70.21, 69.93, 68.27, 52.69. *m/z*: 442 (M^+), 409, 353, 307, 291, 265, 250, 237, 172, 130, 118, 90, 79, 63. Anal. Calcd for $C_{23}H_{30}N_4O_5$: C, 62.44; H, 6.78; N, 12.67. Found: C, 62.74; H, 6.93; N, 12.92%.

4.1.4. Synthesis of 2-(4-*N*-phenylaza-15-crown-5)-5-(4-pyridyl)-1,3,4-oxadiazole (7). Oxidative cyclization of **5** (0.884 g, 2 mmol) was carried out in a manner described for **6** using $KMnO_4$ (0.884 g). The crude product obtained was purified by SiO_2 column chromatography (eluant: 2% CH_3OH in $CHCl_3$) to furnish the desired product **7** as a pale yellow solid in 55% yield (0.484 g), mp 154–157 °C. IR (KBr, ν, cm^{-1}): 2855, 1610, 1498, 1392, 1200, 1119, 829, 742, 698. ^{1}H NMR (300 MHz, $CDCl_3$): δ 8.82 (d, *J*=9 Hz, 2H), 7.97–7.95 (m, 4H), 6.75 (d, *J*=9 Hz, 2H), 3.80 (t, 4H), 3.70–3.64 (m, 16H). ^{13}C NMR ($CDCl_3$): δ 166.14, 161.63, 150.76, 150.56, 131.46, 128.76, 120.13, 111.48, 110.08, 71.33, 70.33, 70.05, 68.24, 52.75. *m/z*: 440 (M^+), 295, 265, 251, 236, 146, 132, 118, 106, 90, 78, 63. Anal. Calcd for $C_{23}H_{28}N_4O_5$: C, 62.73; H, 6.36; N, 12.73. Found: C, 62.98; H, 6.46; N, 13.03%.

Acknowledgements

Thanks are due to B.R.N.S., Government of India for financial support in the form of research grant 2004/37/29/BRNS.

References and notes

1. Czarnik, A. W. *Fluorescent Chemosensors for Ion and Molecule Recognition*; Czarnik, A. W., Ed.; ACS Symposium Series; American Chemical Society: Washington, DC, 1992; Vol. 538, pp 104–129.
2. Rettig, W.; Lapouyade, R. *Probe Design and Chemical Sensing*; Lakowicz, J. R., Ed.; Topics in Fluorescence Spectroscopy; Plenum: New York, NY and London, 1994; Vol. 4, pp 109–149.
3. For recent reviews: (a) de Silva, A. P.; Gunaratne, H. Q. N.; Gunnlaugsson, T.; Huxley, A. J. M.; McCoy, C. P.; Rademacher, J. T.; Rice, T. E. *Chem. Rev.* **1997**, *97*, 1515; (b) Valeur, B. *Chemosensors of Ion and Molecule Recognition*; Desvergne, J.-P., Czarnik, A. W., Eds.; NATO ASI Series C; Kluwer Academic: Dordrecht, 1997; Vol. 492, p 195; (c)

Rurack, K.; Resch-Genger, U. *Chem. Soc. Rev.* **2002**, *31*, 116; (d) Valeur, B.; Leray, I. *Coord. Chem. Rev.* **2000**, *205*, 3.
4. For selected PET/excimer sensors: (a) Jun, E. J.; Won, H. N.; Kim, J. S.; Lee, K.-H.; Yoon, J. *Tetrahedron Lett.* **2006**, *47*, 4577; (b) Kang, J.; Choi, M.; Kwon, J. Y.; Lee, E. Y.; Yoon, J. *J. Org. Chem.* **2002**, *67*, 4384; (c) Sankaran, N. B.; Banthia, S.; Das, A.; Samanta, A. *New J. Chem.* **2002**, *26*, 1529; (d) Burdette, S. C.; Walkup, G. K.; Spinger, B.; Tsien, R. Y.; Lippard, S. J. *J. Am. Chem. Soc.* **2001**, *123*, 7831; (e) Jiang, P.; Guo, Z. *Coord. Chem. Rev.* **2004**, *248*, 205; (f) Kondo, S.; Kinjo, T.; Yano, Y. *Tetrahedron Lett.* **2005**, *46*, 3183.
5. For coumarin based sensors: (a) Kateinopoulos, H. E. *Curr. Pharm. Des.* **2004**, *10*, 3835; (b) Li, H.; Xie, H.; Wang, P.; Wu, S. *New J. Chem.* **2000**, *24*, 105; (c) Bourson, J.; Pouget, J.; Valeur, B. *J. Phys. Chem.* **1993**, *97*, 4552; (d) Chen, C.-T.; Huang, W.-P. *J. Am. Chem. Soc.* **2002**, *124*, 6246.
6. For styryl based sensors: (a) Letard, J. F.; Lapouyade, R.; Rettig, W. *Pure Appl. Chem.* **1993**, *65*, 1705; (b) Rurack, K.; Rettig, W.; Resch-Genger, U. *Chem. Commun.* **2000**, 407.
7. For benzothiazole based sensors: (a) Rurack, K.; Bricks, J. L.; Reck, G.; Radeglia, R.; Resch-Genger, U. *J. Phys. Chem.* **2000**, *104*, 3087; (b) Mashraqui, S. H.; Kumar, S.; Vashi, D. *J. Inclusion Phenom. Macro. Chem.* **2004**, *48*, 125; (c) Mateeva, N.; Deligeorgiev, T.; Miteva, M. *J. Inclusion Phenom. Mol. Recognit. Chem.* **1994**, *17*, 81; (d) Lednev, I. K.; Hester, R. E.; Moore, J. N. *J. Am. Chem. Soc.* **1997**, *119*, 3456.
8. For 8-hydroxyquinoline based sensors: (a) Mei, Y.; Bentley, P. A.; Wang, W. *Tetrahedron Lett.* **2006**, *47*, 2447; (b) Zhang, L.; Meggers, E. *J. Am. Chem. Soc.* **2005**, *127*, 74; (c) Kawakami, J.; Ohta, M.; Yamauchi, Y.; Ohzeki, K. *Anal. Sci.* **2003**, *19*, 1353; (d) Martins, A. O.; de Silva, E. L.; Laranjeira, M. C. M.; de Favere, V. T. *Microchim. Acta* **2005**, *150*, 27; (e) Zhang, H.; Hand, L.-F.; Zachariasse, K. A.; Jiang, Y.-B. *Org. Lett.* **2005**, *7*, 4217; (f) Mei, Y.; Bentley, P. A. *Bioorg. Med. Chem. Lett.* **2006**, *16*, 3131.
9. Mitschke, U.; Bäuerle, P. *J. Mater. Chem.* **2000**, *10*, 1471.
10. Mashraqui, S. H.; Kenny, R. S.; Shailesh, G. G.; Krishnan, A.; Bhattacharya, M.; Das, P. K. *Opt. Mater.* **2004**, *27*, 257.
11. Yang, N. C.; Jeong, J. K.; Suh, D. H. *Chem. Lett.* **2003**, *32*, 40.
12. (a) Tsien, R. Y. *Annu. Rev. Biophys. Bioeng.* **1983**, *12*, 91; (b) Henquin, C.; Tamagawa, T.; Nenquin, M.; Cogneau, M. *Nature* **1983**, *301*, 73; (c) Takahashi, A.; Camacho, P.; Lechleiter, J. D.; Herman, B. *Physiol. Rev.* **1999**, *79*, 1089; (d) Csordas, G.; Hajnoczky, G. *J. Biol. Chem.* **2003**, *278*, 42273; (e) Leite, M. F.; Thrower, E. D.; Echevarria, W.; Koulen, P.; Hirata, K.; Bennett, A. M.; Ehrlich, B. E.; Nathanson, M. H. *Proc. Natl. Acad. Sci. U.S.A.* **2003**, *100*, 2975.
13. Lewis, J. D.; Moore, J. N. *J. Chem. Soc., Dalton Trans.* **2004**, 1376 and references cited therein.
14. Yoshida, K.; Mori, T.; Wanatabe, S.; Kawai, H.; Nagamura, T. *J. Chem. Soc., Perkin Trans. 2* **1999**, 393.
15. Rurack, K.; Bricks, J. L.; Kachkovski, A.; Resch, U. *J. Fluoresc.* **1997**, *7*, 63S.
16. Jonker, A.; Ariese, F.; Verhoeven, J. W. *Recl. Trav. Chim. Pays-Bas* **1989**, *108*, 109.
17. Dix, J. P.; Vögtle, F. *Chem. Ber.* **1980**, *113*, 457.
18. Reddy, P. S. N.; Reddy, P. *Indian J. Chem., Sect. B* **1987**, *26*, 890.
19. Valeur, B. *Molecular Luminescence Spectroscopy*; Schulman, S. G., Ed.; Wiley: New York, NY, 1993; Part 3, pp 25–84.
20. Valeur, B.; Bourson, J.; Pouget, J. *Fluorescent Chemosensors for Ion and Molecular Recognition*; Czarnik, A. W., Ed.; ACS Symposium Series; American Chemical Society: Washington, DC, 1993; Vol. 538, pp 25–44.
21. Brzezinski, B.; Schroeder, G.; Rabold, A.; Zundel, G. *J. Phys. Chem.* **1995**, *99*, 8519.
22. Gunnlaugsson, T.; Leonard, J. P. *J. Chem. Soc., Perkin Trans. 2* **2002**, 1980.
23. Gunnlaugsson, T.; Nieuwenhuyzen, M.; Richard, L.; Thoss, V. *J. Chem. Soc., Perkin Trans. 2* **2002**, 141.
24. Andon, R. J. L.; Cox, J. D.; Herington, E. F. G. *Trans. Faraday Soc.* **1954**, *50*, 918.
25. Meetwa, N.; Enchev, V.; Antonov, L.; Deligeorgiev, T.; Mitewa, M. *J. Inclusion Phenom. Mol. Recognit. Chem.* **1995**, *20*, 323.
26. Jones, G., II; Jackson, W. R.; Choi, C.-Y.; Bergmark, W. R. *J. Phys. Chem.* **1985**, *89*, 294.
27. Rettig, W. *Top. Curr. Chem.* **1994**, *169*, 165.
28. Rurack, K.; Dekhtyar, M. L.; Bricks, J. L.; Resch-Genger, U.; Rettig, W. *J. Phys. Chem. A* **1999**, *103*, 9626.
29. (a) Dey, J. K.; Dogra, S. K. *Bull. Chem. Soc. Jpn.* **1991**, *64*, 3142; (b) Petkov, I.; Deligeorgiev, T.; Timtcheva, I. *Dyes Pigments* **1997**, *35*, 171.
30. Löhr, H. G.; Vögtle, G. *Acc. Chem. Res.* **1985**, *18*, 65.
31. Fery-Forgues, S.; Le Bris, M. T.; Guette, J. P.; Valeur, B. *J. Phys. Chem.* **1988**, *92*, 6233.
32. Mohanty, J.; Bhasikuttan, A. C.; Nau, W. M.; Pal, H. *J. Phys. Chem. B* **2006**, *110*, 5132.
33. Pedersen, C. J.; Frendsdorff, H. K. *Angew. Chem., Int. Ed. Engl.* **1972**, *11*, 16.
34. Pacey, G. E.; Wu, Y. P. *Talanta* **1984**, *31*, 165.
35. Bourson, J.; Valeur, B. *J. Phys. Chem.* **1989**, *93*, 3871.
36. Mathevet, R.; Jonusauskas, G.; Rulliere, C.; Letard, J.-F.; Lapouyade, R. *J. Phys. Chem.* **1995**, *9*, 15709.
37. Chattopadhyay, N.; Serpa, C.; Pereira, M. M.; de Melo, J. S.; Arnaut, L. G.; Formosinho, S. J. *J. Phys. Chem. A* **2001**, *105*, 10025.
38. Kosower, E. M. *Acc. Chem. Res.* **1982**, *15*, 259.
39. Siebrand, W. *J. Phys. Chem.* **1967**, *47*, 2441.
40. Siebrand, W. *J. Chem. Phys.* **1967**, *46*, 440.
41. Lee, D. W.; Kwon, K.-Y.; Jung, J., II; Park, Y.; Kim, Y.-R.; Hwang, I.-W. *Chem. Mater.* **2001**, *13*, 565.